Lawrence Berkeley National Laboratory
LBL Publications

Title

Towards district scale flood simulations using conventional and anisotropic porosity shallow water models with high-resolution topographic information

Permalink

https://escholarship.org/uc/item/4zg6t30k

Journal

La Houille Blanche, 104(2)

ISSN

0018-6368

Authors

Özgen, Ilhan
Abily, Morgan
Zhao, Jiaheng
et al.

Publication Date

2018-04-01

DOI

10.1051/lhb/2018023

Peer reviewed

eScholarship.org Powered by the California Digital Library
University of California

Towards district scale flood simulations using anisotropic porosity shallow water models with high-resolution topographic information

Towards urban flood simulation with conventional and anisotropic porosity models on high resolution topographic data

Ilhan Özgen [1*] , Morgan Abily [2] , Jiaheng Zhao [1] , Dongfang Liang [3] , Philippe Gourbesville [2] and Reinhard Hinkelmann [1]

[1] Chair of Water Resources Management and Modeling of Hydrosystems, Technische Universität Berlin, Germany
[2] Innovative CiTy Lab URE 005, University of Nice Sophia Antipolis (UNS), France
[3] Department of Engineering, University of Cambridge, United Kingdom

[*] ilhan.oezgen@wahyd.tu-berlin.de

Abstract

Current topographic survey provides high-resolution (HR) datasets for urban environments. Incorporating this information is provided in the form of flood forecasting, ie buildings, bridges and street networks. Conceptual, numerical and practical challenges arise from the application of shallow water models to HR urban flood modeling. For instance, numerical challenges are occurrences of wet-dry fronts, geometric discontinuities in the urban environment, and discontinuous solutions, ie shock waves. These challenges can be overcome by using a Godunov-type scheme. However, the computational cost of this type of schemes is high, such that HR two-dimensional shallow water simulations with practical relevance to be run on supercomputers. The porous shallow water model is an alternative approach that aims to reduce computational cost by using a coarse resolution and accounting method. Usually, a speedup between two and three orders of magnitude in comparison to HR simulations can be obtained. This study reports preliminary results of a practical test case concerning flooding in a district of the city of Nice, France, caused by the intense rainfall event on October 3rd 2015. HR topography data set on a resolution is available for the district , the street features of infra-metric dimensions have been included. A reference solution is calculated by HR shallow water model on a 1 m by 1 m structured computational grid. The porous shallow water model is 10 m by 10 m grid and the influence of the drag source is studied. The model results show a large deviation, which is caused by the poor meshing strategy of the porous shallow water (AP) model. The study also summarizes practical challenges that arise during the application of AP and HR models to a large urban catchment. The main difficulty is to obtain a good mesh. In smaller scale investigations, the mesh is currently being constructed by hand such that the cell edges align with buildings. This approach is not feasible for large scale urban buildings with a large number of buildings. Future steps that

have been taken, such as a strategy for automatic mesh generation, are reported on.

Key-words: anisotropic porosity, shallow water model, urban area, FullSWOF_2D, hms, Nice

I. INTRODUCTION

Significant improvement in survey technology during the last decade has increased the availability and accuracy of topography data [Gourbesville, 2009]. These high-resolution (HR) topographic data sets indeed offer promising detailed information of the topographical component of the urban system which itself is a multiscale system, which means that processes occur at different spatial and temporal scale. Small scale features such as buildings and street networks influence the global flow field significantly by creating preferential flow paths. Consequently, decision makers (e.g. at municipal levels) are expecting flood risk professionals to take advantage of these data sets, including them in urban flood risk assessment studies. Both decision makers and flood risk assessment practitioners expect improvement for short- and mid- to long-term risk management such as crisis management and urban planning.

However, incorporating these HR data sets in urban flood models is challenging in terms of data handling and computational cost. HR data sets of urban districts tend to be large, which makes the analysis and preparation of data complicated. Standard meshing techniques such as the Delaunay triangulation might suffer from being over-constrained when HR data sets are used, or require data interpolation from the measurement points to the cell centroids (in a cell-centered finite-volume framework) or to the cell vertices (in a finite-element framework). These difficulties result in mesh quality degradation, which might increase the computation quality and efficency. Structured grids also suffer from interpolation uncertainty if their resolution is coarser than the HR data set. However, running the simulation on the spatial resolution of the data set is also constrained due to the high computational cost such that HR simulations on district scale are feasible only on supercomputers [Abily et al., 2015], [Smith, Liang, 2013].

In literature, various methodologies have been developed to address the issue of computational cost, which can be grouped in three categories: (1) high-performance scientific computing, (2) adaptive methods and (3) reduced modeling. High-performance scientific computing aims to reduce the wall-time of the simulation by means of parallelization, vectorization techniques and specialized computer architecture. The parallelization strategy that is considered to yield the best speedup is the distributed memory parallelization with a message passing interface, as this is known to scale over a large number of processors [Hinkelmann, 2005]. Very recently, the possibility of parallel computation on graphical processor units (GPUs) has been investigated [Smith, Liang, 2013], [Lacasta et al., 2014]. The most common adaptive method in shallow water modeling is the so-called h-

adaptivity, which adjusts the mesh resolution automatically to capture regions that are identified as critical, e.g. the region around a propagating shock wave is automatically refined while smooth areas are coarsened. The adjustment is usually steered by an error-estimator, which is for example related to the gradient of the flow field [Hinkelmann, 2005]. Reduced modeling comprises reduced complexity modeling, which uses simplified governing equations to describe the water movement [McMillan, Brasington, 2007] and coarse grid approaches, which run simulations on a coarser resolution and account for subgrid-scale information by means of conceptual approaches. A well-known reduced complexity method is the diffusive wave approximation of the shallow water equations that neglects local inertia terms, e.g. [Jahanbazi et al., 2017]. An example for the coarse grid approach would be the porous shallow water equations, e.g. [Guinot, Soares-Frazão, 2006].

The porous shallow water equations have been derived in various ways. The earliest appearance of the equations is found in [Defina, 1994] and the first published application to urban systems is found in [Hervouet, 2000]. The porosity is defined in each cell as the fraction of the cell available to flow, i.e. not occupied by obstacles. Important contribution to the numerical modeling approach has been presented in [Guinot, Soares-Frazão, 2006], [Soares-Frazão et al., 2008]. A limitation of these porous shallow water model is their inability to represent directionality due to building geometry. Thus, preferential flow paths could not be reproduced accurately [Guinot, 2012]. [Sanders et al., 2008] present an anisotropic porosity model that overcomes this limitation by defining additional porosity terms at the cell edges that represent the fraction of the edge that is available to flow. These edge porosities are able to block and divert the flow, hence introducing directionality to the model. Similar approaches are suggested in [Lhomme, 2006] for the single porosity model by [Guinot, Soares-Frazão, 2006] and [Chen et al., 2012a], [Chen et al., 2012b] for a diffusive wave model. The porous shallow water models have been validated at laboratory scale and have shown to produce results with comparable accuracy to the conventional shallow water model [Kim et al., 2014]. However, local flow details can not be reproduced using these type of models.

This contribution aims to give an introduction of the methodology of the anisotropic porosity model and to point out challenges that occur when applying the anisotropic porosity model at district scale. Most applications of the anisotropic porosity model are at laboratory scale, e.g. [Sanders et al., 2008], [Kim et al., 2014], [Kim et al., 2015], [Özgen et al., 2016a], [Özgen et al., 2016b]. An exception is the levee-break flood modeling case presented in [Guinot et al., 2017] which considers a real-world application, however at a much smaller scale than the test case investigated herein, i.e. the domain in [Guinot et al., 2017] spans less than 1 km², while the domain in this work spans about 5 km². Prelimiary results are presented and compared with a reference solution obtained by a HR simulation with a model which solves

the conventional shallow water equations: FullSWOF_2D [Delestre et al., 2014].

II. MATHEMATICAL AND NUMERICAL MODEL CONCEPTS

II.1. Conventional shallow water equations for high-resolution modeling

The conventional two-dimensional shallow water equations can directly be derived from the continuity and Navier-Stokes equations by depth-integrating them under the assumption of incompressibility, free water surface, small slopes and negligible vertical acceleration and viscous forces [Hinkelmann, 2005]. This gives a balance law of the form

$$\frac{\partial}{\partial t}\int_{\Omega}\mathbf{q}\,d\Omega+\oint_{\partial\Omega}\mathbf{F}\mathbf{n}\,dr=\int_{\Omega}\mathbf{s}\,d\Omega, \qquad (1)$$

where t is the time, Ω is the area of the control volume, ∂Ω is the boundary of the control volume, *r* is the path along the boundary in counter-clockwise direction, **q** is the vector of conserved variables, **F** is the flux vector, **n** is the unit normal vector pointing outwards of the control volume and s is the source vector. The vectors are written as

$$\mathbf{q}=\begin{bmatrix}h\\ uh\\ vh\end{bmatrix};\ \mathbf{F}=\begin{bmatrix}uh & vh\\ u^2h+\frac{1}{2}gh^2 & uvh\\ uvh & v^2h+\frac{1}{2}gh^2\end{bmatrix};\ \mathbf{s}=\begin{bmatrix}m\\ -\left(c_D^f+c_D^b\right)u\|\mathbf{v}\|+s_{bx}\\ -\left(c_D^f+c_D^b\right)v\|\mathbf{v}\|+s_{by}\end{bmatrix} \qquad (2)$$

with *h* standing for the water depth, *u* and *v* standing for the velocities in *x*- and *y*-direction, respectively, whereby *x* and *y* are the axes of the Cartesian coordinate system, *g* is the gravity, **m** is the mass source term that is for example a rainfall intensity, c_D^f is the friction coefficient, c_D^b is the drag coefficient, ||**v**|| denotes the Euclidian norm of the vector of velocities, i.e. **v**=[*u*; *v*]^T and s_{bx} and s_{by} are the bottom slope source terms in *x*- and *y*-direction, respectively, calculated as

$$s_{bx}=-gh\frac{\partial z}{\partial x};\ s_{by}=-gh\frac{\partial z}{\partial y}, \qquad (3)$$

where *z* is the bottom elevation. In this work, Manning's law is used to calculate the friction coefficient as

$c_D^f = gn^2h^{-1/3}$ and the drag coefficient is calculated as $c_D^b = 0.5\,c_D^0\,h$.

II.2. Shallow water equations with anisotropic porosity for coarse grid modeling

For the derivation of the shallow water equations with anisotropic porosity, the phase function *i* is introduced, which is defined as equal to 0 in the solid areas, and 1 in the water region [Sanders et al., 2008]. Each term in Eq. (1) is multiplied with *i* to obtain a new balance law:

$$\int_{\Omega} i\mathbf{q}d\Omega + \oint_{\partial\Omega} i\mathbf{F}\mathbf{n}dr = \oint_{\Omega} i\mathbf{s}d\Omega + \oint_{\Gamma} i\mathbf{H}\mathbf{m}dr \qquad (4)$$

Here, q, F and s are the same as in Eq. (2). An additional term **H** appears in the equations that accounts for unresolved solid-water interaction, that is integrated over the path Γ, which denotes the interface boundary between solid and water. **m** is the unit normal vector pointing outwards of the water phase. Because this process can not be resolved explicitly with the chosen size of the control volume (Ω), a closure for this term is needed. A common approach is to split the integral in two components: the stationary and the non-stationary component. The non-stationary component is then calculated using a drag formulation and this already appears in the vector **s** in $c_D{}^b$, cf. Eq. (2). The stationary component is discretized as

$$\oint_{\Gamma} i(\mathbf{H}\mathbf{m})^{nst} dr = \oint_{\partial\Omega} i(\mathbf{H}\mathbf{n}) dr, \qquad (5)$$

with

$$\mathbf{H} = \begin{bmatrix} 0 & 0 \\ \frac{1}{2}gh|_{\eta_0}^2 & 0 \\ 0 & \frac{1}{2}gh|_{\eta_0}^2 \end{bmatrix}, \qquad (6)$$

which means that the influence of **H** is shifted from the solid-fluid interface to the control volume boundary (Eq. (5)) and approximated with a hydrostatic pressure term that depends on an average water depth $h|_{\eta 0}$ evaluated for a constant water elevation inside the cell. Sanders et al. [2008] proposed this closure for a cell-centered Godunov-type finite-volume method where bed elevations are defined at the vertices of the cell [Begnudelli et al., 2008]. This scheme discretizes a continuous topography at cell edges, i.e. no topography discontinuity at the edges is allowed. This type of topography discretization is advantageous for the solution of the Riemann problem across the edge but bears numerical challenges at wet-dry fronts [Fišer et al., 2016]. Özgen et al. [2016] show that this closure is also valid for a conventional cell-centered Godunov-type finite-volume discretization that uses the hydrostatic reconstruction [Audusse et al., 2004].

Porosity terms are now defined as

$$\phi_j = \frac{1}{\Omega_j}\int_{\Omega_j} id\Omega; \quad \psi_k = \frac{1}{\partial\Omega}\int_{\partial\Omega} idr, \qquad (7)$$

where ϕ_j is the volumetric porosity calculated in each cell j, and ψ_k is the areal porosity calculated at each edge k. The phase function i connects the subgrid-scale topography with the porosities and therefore incorporates the HR data set conceptually into the coarse grid model.

Carrying out the discrete integration in Eq. (4) yields the explicit finite-volume formulation as

$$(\phi\mathbf{q})^{n+1} = (\phi\mathbf{q})^{n} + \frac{\Delta t}{\Omega}\left(\sum(\psi\mathbf{Fn} - \psi\mathbf{Hn})_k^n \Delta k - \phi\mathbf{s}\right), \quad (8)$$

instead of the conventional finite-volume formulation that results from integrating Eq. (1):

$$\mathbf{q}^{n+1} = \mathbf{q}^{n} + \frac{\Delta t}{\Omega}\left(\sum(\mathbf{Fn})_k^n \Delta k - \mathbf{s}\right) \quad (9)$$

Here, n denotes the time level, Δt is the time step size and Δk is the edge length.

II.3. Numerical model

The conventional shallow water equations solution are implemented in FullSWOF_2D, a C++-based finite-volume code mainly developed at the Université d'Orléans [Delestre et al., 2014] and the referenced high resolution work and results come from the Université Nice Sophia Antipolis work on FullSWOF_2D. The anisotropic porosity shallow water equations are implemented in the Hydroinformatics Modeling System (hms), a Java-based finite-volume code developed at the Chair of Water Resources Management and Modeling of Hydrosystems, Technische Universität Berlin [Simons et al., 2014].

Both numerical models are very similar, as they are Godunov-type finite-volume methods [Godunov, 1956] which apply a MUSCL reconstruction [van Leer, 1979] to achieve second order of accuracy and utilize an approximate Riemann solver of the contact wave restored Harten, Lax and van Leer-type (HLLC) [Toro et al., 1994] to calculate the numerical flux. The hydrostatic reconstruction [Audusse et al., 2004] is used to preserve the C-property.

FullSWOF_2D solves Eq. (9) and hms solves Eq. (8). It is noted that hms is usually applied to solve the conventional shallow water equations, i.e. Eq. (9), and that the results reported in the following sections are produced by an experimental module of hms called hms-pp.

II.3.1. Discussion of the inclusion of HR features in the conventional shallow water model

Optimal use of high-resolution topographic information such as modern photo-interpreted datasets in standard 2D numerical modelling tools might be challenging in terms of data integration. The Preconceived idea is that photo-interpreted dataset might be efficient for non-structured mesh

generation as the data is under a vectorized format which should offer interesting possibilities for non-structured mesh generation. In practice, for HR urban flood modeling, structured grid meshes allow to apply simple methodologies to include inframetic above-ground features which influence flood flow paths and elevation calculation (e.g. buildings, urban walls, sidewalks, etc.) where standard non-structured meshing algorithm (e.g. advancing front method, Delaunay and constrained Delaunay triangulation methods) fail due to over constraint and quick changes in topographic gradient [Abily et al., 2015]. As a reminder, two main disadvantages arise however from the use of structured mesh. First the regular size of elements implies that the highest mesh resolution one can expect from the discretization procedure is the same over the domain. Hence, in areas where the physical properties of the phenomena wished to be modelled, or where the variable (elevation) does not vary, there will be an unnecessary over-discretization of the domain. Consequently it will involve a high computational cost along with the storage of potentially unnecessary information. Here, the use of a High-Performance Computing (HPC) tends to overcome this issue. Second, disadvantage of a structured Cartesian mesh is that if the flow or any singularity is orientated, in the worst case, plus or minus 45° compared to the *x*- or *y*-direction, the computation will artificially go through a stepwise zig-zag processing [Ma et al., 2015]. As a result, the number of cells, and therefore the length over which the water will flow, is artificially increased by this process.

FullSWOF_2D uses Cartesian structured meshing approach. When dealing with HR topographic dataset, advantage is that that the DEM representing the domain can be used as a computational grid following a straight forward format conversion. However, this assumes that the digital elevation model (DEM) representing the domains considered as already suited for the HR hydraulic modelling application.

The interest of photo-interpreted datasets for the hydraulic community is that it allows to build a HR DEM that encompasses fine features that can be selected by the modeler for its purpose, depending on the level of complexity of features that the modeler judges relevant to include [Abily et al., 2016], [Salvan et al., 2016]. It should be noted that this judgment is based on expert opinion only and an analysis of the effects of the level of complexity of features included in the model depends on the purpose. In this study, classes of above-ground features that have been considered as introducing complexity in surface drainage paths were selected. The classes of selected features (under vector form) were converted to raster and extruded on the DEM at a 1m-resolution.

II.3.2. Discussion of the calculation of the porosity terms in the anisotropic porosity shallow water model

Porosities are calculated individually in each cell and at each edge by means of sampling the HR data set in each cell. The number of sample points is

determined by the modeler and the recommended number depends on the mesh type and the complexity of the HR data set.

First, consider a structured grid with aligned subgrid-scale buildings as shown in the top view sketch of a computational cell in Fig. (1) (left). The grey blocks represent the buildings, the thick black line is the boundary of the computational cell and the thin black lines show the sampling resolution, which is denoted with Δh. Traversing the HR data set located inside the cell, simply counting the sample points that have their centroids located at a void and dividing by the total number of sample points gives the volumetric porosity ϕ. In the illustrated case this corresponds to

$$\phi = \frac{58}{121}. \qquad (10)$$

It is apparent from Fig. (1), that the porosity calculation is exact and that refining the sampling resolution will not change the value of the porosity. If the sample resolution is coarsened, i.e. Δh increases, the value of ϕ changes. This suggests that there is some kind of grid convergence for the sampling resolution that has to be reached to obtain reliable results, which is reached on structured grids with aligned buildings at a relative coarse sampling resolution.

For non-aligned buildings with structured grids, the grid convergence of the sampling resolution can be reached only at much smaller Δh. The nature of the problem can be understood clearly by considering the case illustrated in Fig. (1) (right). If the porosity is calculated based on the illustrated sampling resolution, the volumetric porosity ϕ does not correspond to the exact analytical value. If the sample size is decreased to $\Delta h/2$, which means that the sample number increases by the power of 2, the value of ϕ changes and becomes more exact. As Δh decreases, the value of ϕ becomes more accurate until the discrete calculation converges to the analytical calculation.

Obviously, as the number of sample points increases the computational cost of this step increases. This is not a serious drawback, as the porosity values should be calculated only once in a pre-processing step, but should be kept in mind.

For triangular cells, the sampling gets in theory more complicated. In a triangular cell, sample points should not contribute equally to the porosity calculation but should be multiplied with weights that correspond to the subarea in the cell that they represent. In analogy to the Thiessen polygon interpolation used in hydrology and other fields, it is proposed to carry out a Voronoi tessellation of the computational cell based on all available HR data points and use the area of the resulting Thiessen polygons as weights for the corresponding sample in the porosity calculation. A less complicated way is to apply a brute-force approach as reported in [Guinot et al., 2017], where porosities are calculated using 10000 sample points in a triangular cell. In this case with such a large sample number, the weights become negligible.

Considerations of the computational cost in the pre-processing step as discussed above still apply.

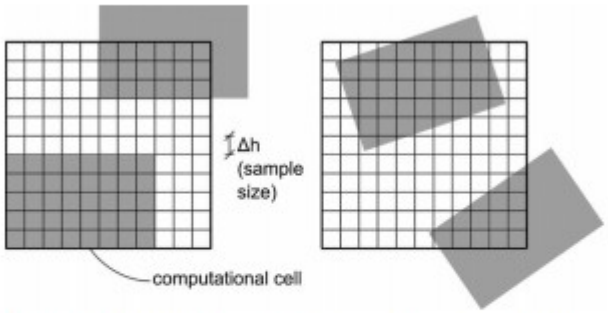

Figure 1: *Top view sketch of two possible cell and building configurations: aligned configuration (left) and non-aligned configuration (right). Grey blocks represent buildings, thick black lines represent the cell boundary, thin black lines show the sampling resolution.*

III. PRELIMINARY RESULTS: DISTRICT SCALE PLUVIAL FLOOD MODELING IN NICE, FRANCE

The aim of this case study is to apply the anisotropic porosity shallow water model to a “real world” case with typical scales for urban flood modeling problems to identify potential limitations of the model. The simulated event is an urban flooding case generated by an intense rainfall event on October 3rd, 2015. Results of the anisotropic porosity shallow water model (hms-pp) are compared with results obtained by a high-resolution conventional shallow water model (FullSWOF_2D).

III.1. Study site and modeled flood event

The study site is an approximately 5 km2 spanning district of the city of Nice, France. The topography information is based on a DEM with 1m resolution, which includes infra-metric structures. A three-dimensional plot of the DEM is shown in Fig. (2). Here, the buildings have been artificially heightened for illustration purposes.

To create the HR DEM, the following approach has been carried out: firstly, a DEM was created, using multiple ground level information at a 0.5 m resolution by the municipality. Then, a selection procedure among classes of photo-interpreted data was performed. This selection is achieved by considering features that can influence overland flow drainage paths [Salvan et al., 2016]. It includes buildings and walls. During this step, information on elevated roads and bridges which might block overland flow paths were removed. Fine features were included in a 1 m resolution DEM by over sizing their horizontal extent to 1 m. The resulting HR DEM represents a 3.2 km² urban area, with its longest flow path of 4.5 km through a problematic location under a bridge (St. Augustin Bridge), located in a retention area often flooded during intense rainfall events (Fig. (3)).

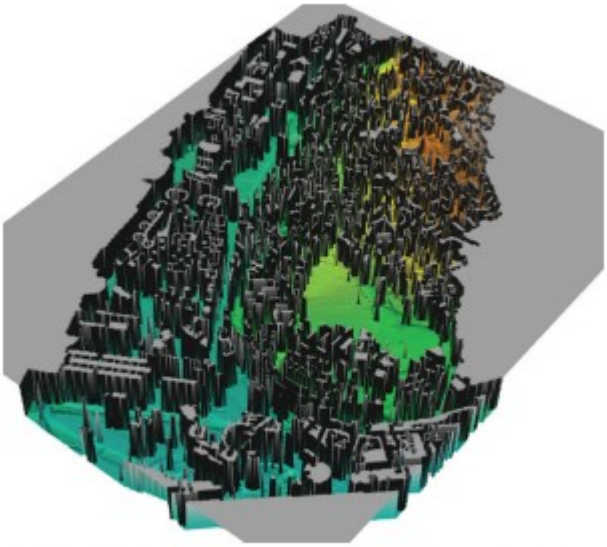

Figure 2: *Three-dimensional plot of the digital elevation model of the domain with overelevated buildings.*

Figure 3: *Overview of the downstream part of the urban catchment (left) with picture of the maximum water level reached on the 3rd October, 2015, at St. Augustin Bridge (center) and the maximum water levels computed with FullSWOFF_2D at this area (right).*

III.2. Numerical parameters and computational aspects

Abily [2015] and Abily et al. [2016] give a detailed discussion on the creation of the DEM and HR simulations in the area using FullSWOF_2D, where a spatially uniform Manning friction coefficient of $n = 0.0166$ $sm^{-1/3}$ is determined, which corresponds approximately to the roughness of old concrete and thus lays in an appropriate range. This value is also used in the anisotropic porosity shallow water model and no further calibration of the friction coefficient has been carried out. However, the anisotropic porosity shallow water model is calibrated using the drag coefficient.

Initially, the whole domain is considered dry. The flood event is created by imposing a 3 h long, spatially uniform rainfall event from a recorded time series with 2 min resolution shown in Fig. (4). A maximum intensity of about $2.5 \bullet 10^{-5}$ m/s, which is about 96 mm/h, is measured between 0.85 h and 1.2 h. All boundaries are considered closed boundaries. This is consistent with

the simulation runs carried out with FullSWOF_2D [Abily et al., 2016]. The total simulation duration is 10800 s (3 h).

The high-resolution model discretizes the domain with a 1m resolution, which results in a mesh with 5,906,844 cells. The model runs parallel on 128 CPUs, taking about 16 h wall-time to finish. The anisotropic porosity shallow water model discretizes the domain with 10 m by 10 m cells, resulting in 59,068 cells. The anisotropic porosity shallow water model runs parallel on 32 CPUs and requires about 1 h wall-time to finish.

Simulations on different resolutions, namely 25 m by 25 m and 50 m by 50 m cells, are planned in future research. Fig. (5) shows the effect of grid coarsening in the area, using the aforementioned cell sizes. The 1 m resolution is the reference case. It is seen that in a 10 m resolution, several buildings are still explicitly represented and the overall characteristics of the urban catchment is reproduced. Increasing the resolution up to 20 m makes most of the buildings disappear. Finally, at 50 m resolution, the buildings and streets have completely disappeared.

Porosities are calculated by means of sampling the HR data set as discussed above. Here, the sampling takes place at the HR data set resolution, i.e. Δh = 1 m, 100 sample points per cell. Buildings are artificially overelevated to 190 m in the DEM. Thus, if the sample exceeds a threshold of 170 m, the sample is considered to lay at a building.

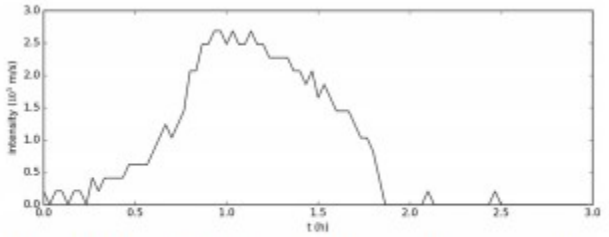

Figure 4: *Plot of the input rainfall event that generated the Nice flood of October 3rd, 2015.*

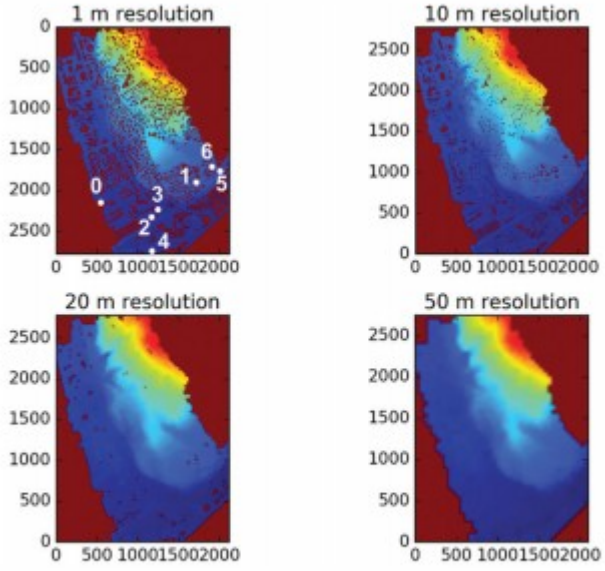

Figure 5: *Digital elevation models of the study area with different spatial resolutions.*

III.3. Results

In a first preliminary study, the influence of the drag coefficient is assessed. Two simulation runs are carried out, whereby the first simulation run neglects the head loss due to drag, i.e. cD 0 = 0. In the second simulation run, the drag coefficient is set to $c_D^0 = 5$ m^2.

Results of the high-resolution simulation (reference) and the anisotropic porosity shallow water model (AP) are compared at 6 virtual gauges located inside the domain. The comparison is for $c_D^0 = 0$ is plotted in Fig. (6). The agreement between both models is poor, except at gauge 1 where reasonable agreement is observed. At gauges 2 and 3, the HR model produces no water depth because these gauges are located on buildings. Because the AP model uses a coarser resolution, these gauges lay inside a cell that is not identified as a building anymore and thus a water depth is calculated here. In theory, this error could be filtered out by mapping the water depth back to the HR data set, but it shows a limitation of the AP model. Water depths at gauge 4 are overestimated, while water depths at gauge 5 are underestimated.

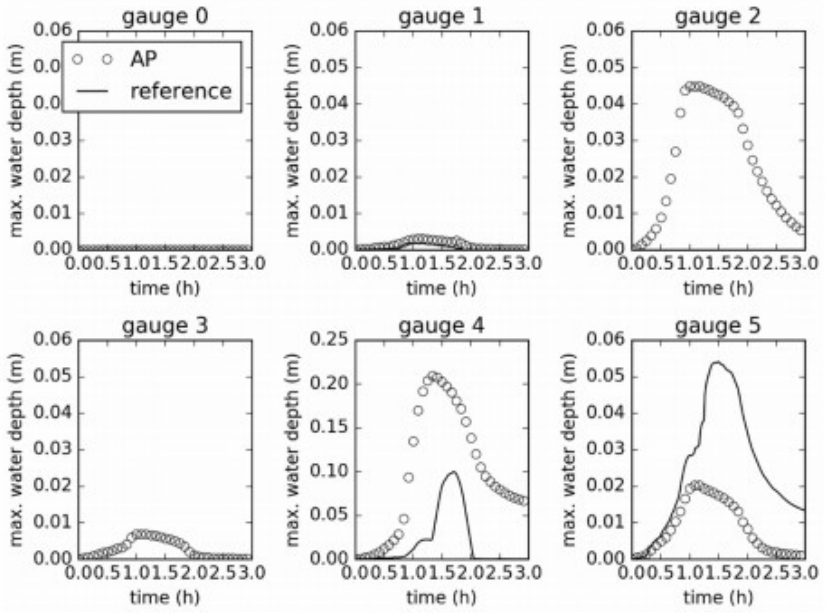

Figure 6: *Comparison of computed water depths at 6 gauges for the AP model using 10 m resolution without drag induced head losses and the HR reference model.*

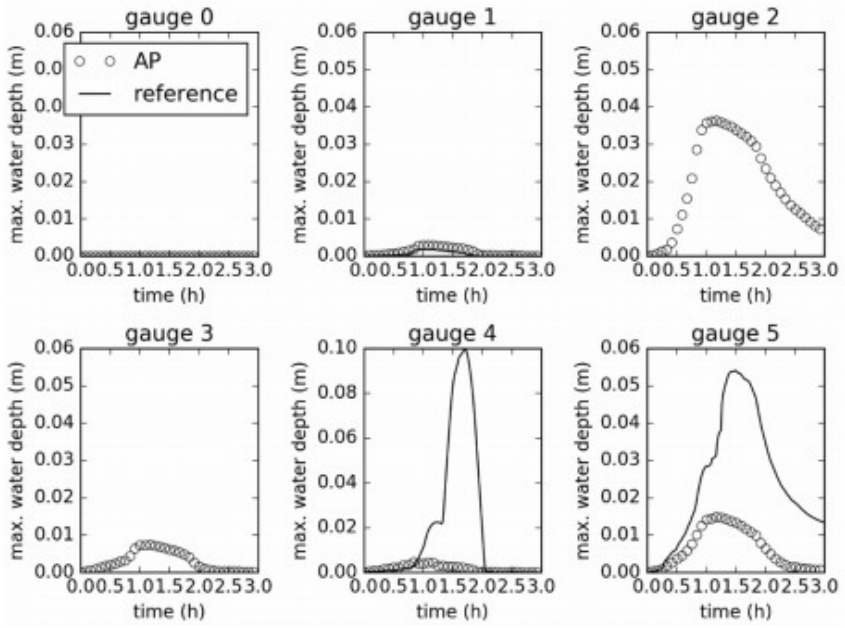

Figure 7: *Comparison of computed water depths at 6 gauges for the AP model using 10 m resolution with drag coefficient c_D^0=5 m² and the HR reference model.*

Fig. (7) shows a comparison of the results for the simulation run with $c_D^0 = 5$ m^2. The most significant effect is observed at gauge 4, where the water depth decreases significantly. Other gauges seem not effected as much. Overall, the agreement between the results is still poor.

III.4. Discussion of preliminary results and practical aspects

The present study shows large deviations between both model concepts. As the results of the anisotropic porosity shallow water model are mesh-dependent, this is most likely due to the poor meshing strategy followed in this study. As pointed out in [Özgen et al., 2016], structured grids should be constructed such that ideally the cell edges align with building edges. This can be achieved in laboratory scale studies with idealized urban geometry, such as the experiments reported in [Testa et al., 2010], [Soares-Frazão, Zech, 2008], but is difficult to apply in a complex real world urban catchment. Thus, an important conclusion to be drawn is that structured grids pose a severe limitation to the model accuracy for the porous shallow water model and consequently, it is recommended to use unstructured triangular meshes in future studies.

Overall, the preliminary results are sobering. Maximum water depths computed by the HR model could not be reproduced by the AP model. The temporal evolution of the water depths at the gauges is also not reproduced correctly. For the simulation run $c_D{}^0 = 5\ m^2$, the first hour of the simulation shows reasonable agreement at gauge 4 and gauge 5 but then fails to reproduce the peaks in the hydrographs.

The anisotropic porosity shallow water model with unstructured triangular meshes has been studied in [Sanders et al., 2008], [Kim et al., 2014], [Kim et al., 2015]. Here, [Kim et al., 2014] report excellent agreement and an accuracy similar to the conventional high-resolution shallow water model if the meshing is carried out appropriately. For unstructured grids, [Kim et al., 2014] reported the optimal meshing strategy to be gap-conforming meshes, i.e. cell vertices are located at the centroids of the buildings.

In both cases, while for small-scale investigations with few buildings the modeler may create such meshes by hand, for large scale investigations this approach is not desirable. Thus, automatic meshing algorithms need to be addressed in future research concerning district scale applications.

III.4.1. Practical challenges of the high-resolution shallow water model

To summarize the main challenges related to the HR modeling of an intense rainfall event generating a flood event over an urban area, it is important to point out that: the use of structured grid approach is straight forward but requires HPC resources; the use of a HR DEM is subject to the modeler assessment of relevance of data that she or he choses to implement in the HR DEM; high gradient occurrences (e.g. walls) in theory violate the validity of models relying on shallow water equations solution approximation near by them; added value of fine features inclusion in DEM is clearly observed disregarding resolution used for their inclusion (oversizing inframetric flow structurant elements to a 1m resolution); fully impermeability/discontinuity related to process used for fine features inclusion can reach its limit by creating artificial discontinuities in the hydrodynamics of the flood.

III.4.2. Practical challenges of the anisotropic porosity shallow water model

As discussed above, the main challenge of applying the anisotropic porosity shallow water model at district scale is to generate a gap-conforming mesh. Such a mesh could be generated by an automatic mesh generation algorithm that takes a list of polygons which describe the building boundaries as input. The polygons could be determined by means of image analysis tools, e.g. OpenCV [Bradski, Kaehler, 2008]. The algorithm would then determine the centroid of each polygon and perform a constrained Delaunay triangulation, forcing the incorporation of the centroids in the mesh. Such constrained triangulations are available in many mesh generators, e.g. Gmsh [Geuzaine, Remacle, 2009] or Triangle [Shewchuk, 1996].

IV. CONCLUSIONS

A comparison between a conventional high-resolution shallow water model and an anisotropic porosity shallow water model in a district-scale application has been presented. Large deviations between the model results were observed, which can be traced back to the poor mesh choice of the anisotropic porosity shallow water model. Future research will focus on generating a better mesh to increase the model accuracy.

On a final note, FullSWOF_2D is available under the CeCILL-V2 license (GPL compatible) at http://www. univ-orleans.fr/mapmo/soft/FullSWOF.

V. ACKNOWLEDGEMENTS

This work was supported by the DFG Research Training Group “Urban Water Interfaces” (DFG-GRK2032). Photogrammetric and photo-interpreted dataset used for this study have been kindly provided by Nice Côte d’Azur Metropolis for research purpose. This work was granted access to the HPC and visualization resources of the “Centre de Calcul Interactif” hosted by University Nice Sophia Antipolis.

VI. REFERENCES

Abily, M. (2015) — High-resolution modelling with bi-dimensio- nal shallow water equations based codes: high-resolution topographic data use for flood hazard assessment over urban and industrial environments. Doctoral thesis, Université Nice Sophia Antipolis.

Abily, M., Bertrand, N., Delestre, O., Gourbesville, P. & Duluc, C.-M. (2016) — Spatial global sensitivity analysis of high-resolution classified topographic data use in 2D urban flood modelling. Environmental Modelling & Software, 77, 183-195.

Audusse, E., Bouchut, F., Bristeau, M.O., Klein, R. & Perthame, B. (2004) — A fast and stable well-balanced scheme with hydrostatic reconstruction for shallow water flows. SIAM Journal on Scientific Computing, 25, 2050-2065.

Begnudelli, L., Sanders, B.F.& Bradford, S.F. (2008) — An adaptive Godunov-based model for flood simulation. Journal of Hydraulic Engineering, 134, 714-725.

Bradski G.& Kaehler A. (2008) — Learning OpenCV: Computer vision with the OpenCV library. O'Reilly Media, Inc.

Chen, A.S., Evans, B., Djordjević, S. & Savić, D. (2012) — A coarse-grid approach to representing building blockage effects in 2D urban flood modelling. Journal of Hydrology, 426-427, 1-16.

Chen, A.S., Evans, B., Djordjević, S. & Savić, D. (2012) — Multi-layered coarse grid modelling in 2D urban flood simulations. Journal of Hydrology, 470-471, 1-11.

Defina, A., D'Alpaos, D. & Matticchio, B. (1994) — A new set of equations for very shallow flow and partially dry areas suitable to 2D numerical models. Proceedings of the Specialty Conference on "Modelling of Flood Propagation Over Initially Dry Areas", New York, USA, 72-81.

Delestre, O., Cordier, S., Darboux, F., Du, M., James, F., Laguerre, C., Lucas, C., Planchon, O. (2014) — FullSWOF: A software for overland flow simulation. Advances in Hydroinformatics, Eds: Gourbesville, P., Cunge, J., Caignaert, G., Springer-Verlag, Singapore, 221-231.

Fišer, M., Özgen, I., Hinkelmann, R. & Vimmr, J. (2016) — A mass conservative well-balanced reconstruction at wet/ dry interfaces for the Godunov-type shallow water model. International Journal for Numerical Methods in Fluids, 82, 893-908.

Geuzaine, C. & Remacle, J.F. (2009) — Gmsh: a three-dimensional finite element mesh generator with built-in pre- and post-processing facilities. International Journal for Numerical Methods in Engineering, 79, 1309-1331.

Gourbesville, P. (2009) — Data and hydroinformatics: new possibilities and challenges. Journal of Hydroinformatics, 11, 330-343.

Guinot, V. (2012) — Multiple porosity shallow water models for macroscopic modelling of urban floods. Advances in Water Resources, 37, 40-72.

Guinot, V., Sanders, B.F. & Schubert, J.E. (2017) — Dual integral porosity shallow water model for urban flood modelling. Advances in Water Resources, in press.

Guinot, V. & Soares-Frazão, S. (2006) — Flux and source term discretization in two-dimensional shallow water models with porosity on unstructured grids. International Journal for Numerical Methods in Fluids, 50, 309-345.

Hervouet, J.M., Samie, R. & Moreau, B. (2000) — Modelling urban areas in dam-break flood-wave numerical simulations. International Seminar and Workshop on Rescue Actions based on Dambreak Flood Analysis, Vol. 1, Seinâjoki, Finland.

Hinkelmann, R. (2005) — Efficient Numerical Methods and Information-Processing Techniques for Modelling Hydro- and Environmental Systems, Springer-Verlag, Berlin, Heidelberg.

Jahanbazi, M., Özgen, I., Aleixo, R. & Hinkelmann, R. (2017) — Development of a diffusive wave shallow water model with a novel stability condition and other new features. Journal of Hydroinformatics, in press.

Kim, B., Sanders, B.F., Famiglietti, J.S. & Guinot, V. (2015) — Urban flood modelling with porous shallow-water equations: A case study of model errors in the presence of anisotropic porosity. Journal of Hydrology, 523, 680-692.

Kim, B., Sanders, B.F., Schubert, J.E. & Famiglietti, J.S. (2014) — Mesh type tradeoffs in 2D hydrodynamic modeling of flooding with a Godunov-based flow solver. Advances in Water Resources, 68, 42-61.

Lacasta, A., Morales-Hernández, M., Murillo, J. & García-Navarro, P. (2014) — An optimized GPU implementation of a 2D free surface simulation model on unstructured meshes. Advances in Engineering Software, 78, 1-15.

Lhomme, J. (2006) — One-dimensional, two-dimensional and macroscopic approaches to urban flood modelling. Doctoral thesis, Université Montpellier 2.

McMillan, H.K. & Brasington, J. (2007) — Reduced complexity strategies for modelling urban floodplain inundation. Geomorphology, 90, 226-243.

Özgen, I., Liang, D. & Hinkelmann, R. (2016) – Shallow water equations with depth-dependent anisotropic porosity for sub- grid-scale topography, Applied Mathematical Modelling 40, 7447-7473.

Özgen, I., Zhao, J., Liang, D. & Hinkelmann, R. (2016) — Urban flood modelling using shallow water equations with depth-dependent anisotropic porosity. Journal of Hydrology, 541, 1165-1184.

Salvan, L., Abily, M., Gourbesville, P. & Schoorens, J. (2016) — Drainage system and detailed urban topography: towards operational 1D-2D modelling for stormwater management. Proceedia Engineering, 154, 890-897.

Sanders, B.F., Schubert, J.E. & Gallegos, H.A. (2008) — Integral formulation of shallow-water equations with anisotropic porosity for urban flood modeling. Journal of Hydrology, 362, 19-38.

Shewchuk, J.R. (1996) — Triangle: engineering a 2D quality mesh generator and Delaunay triangulator. Applied Computational geometry: towards geometric engineering. Lin, M.C., Manocha D. (eds), Lecture Notes in Computer Science 1148, Springer-Verlag, Berlin Heidelberg, 203-222

Simons, F., Busse, T., Hou, J., Özgen, I. & Hinkelmann, R. (2014) — A model for overland flow and associated processes within the Hydroinformatics Modelling System. Journal of Hydroinformatics, 16, 375-391.

Smith, L.S. & Liang, Q. (2013) — Towards a generalized GPU/ CPU shallow-flow modelling tool. Computers & Fluids, 88, 334-343.

Soares-Frazão, S., Lhomme, J., Guinot, V. & Zech, Y. (2008) — Two-dimensional shallow-water model with porosity for urban flood modelling. Journal of Hydraulic Research, 46, 45-64.

Soares-Frazão, S. & Zech, Y. (2008) — Dam-break flow through an idealised city. Journal of Hydraulic Research, 46, 648-658.

Testa, G., Zuccalà, D., Alcrudo, F., Mulet, J. & Soares-Frazão, S. (2010) — Flash flood flow experiment in a simplified urban district. Journal of Hydraulic Research, 45, 37-44.

Toro, E.F., Spruce, M. & Speares, W. (1994) — Restoration of the contact surface in the HLL-Riemann solver. Shock Waves, 4, 25-34.

van Leer, B. (1979) — Towards the ultimate conservative difference scheme. V. A second-order sequel to Godunov’s method. Journal of Computational Physics, 32, 101-136.